Photochemistry and Photobiology, 2014, 90: 121–128

Synthesis of Zinc Chlorophyll Homo/Hetero-Dyads and their Folded Conformers with Porphyrin, Chlorin, and Bacteriochlorin π-Systems

Hitoshi Tamiaki*, Kazuhiro Fukai, Hideki Shimazu and Sunao Shoji

Graduate School of Life Sciences, Ritsumeikan University, Shiga, Japan

Received 5 August 2013, accepted 4 September 2013, DOI: 10.1111/php.12173

ABSTRACT

Zinc complex of pyropheophorbide-*b*, a derivative of chlorophyll-*b*, was covalently dimerized through ethylene glycol diester. The synthetic homo-dyad was axially ligated with two methanol molecules from the *β*-face and both the diastereomerically coordinating methanol species were hydrogen bonded with the keto-carbonyl groups of the neighboring chlorin in a complex. The resulting folded conformer in a solution was confirmed by visible, ^{1}H NMR and IR spectra. All the synthetic zinc chlorin homo- and hetero-dyads consisting of pyropheophorbides-*a*, *b* and/or *d* took the above methanol-locked and π–π stacked supramolecules in 1% (v/v) methanol and benzene to give redmost (Qy) electronic absorption band(s) at longer wavelengths than those of the corresponding monomeric chlorin composites. The other zinc chlorin and bacteriochlorin homo-dyads completely formed similar folded conformers in the same solution, while zinc inverse chlorin and porphyrin homo-dyads partially took such supramolecules. The J-type aggregation to folded conformers and the redshift values of composite Qy bands were dependent on the electronic and steric factors of porphyrinoid moieties in dyads.

INTRODUCTION

Close situation (van der Waals contact) of chlorophyll (Chl) molecules is important for construction of photosynthetic apparatus, and π–π stacking of Chl pigments in particular is often observed in light-harvesting and energy-transferring antennas as well as charge separating reaction centers (RCs) (1). In light-harvesting complexes 1 and 2 of purple anoxygenic photosynthetic bacteria, several bacteriochlorophyll(BChl)-*a* and/or *b* molecules interacted with each other through coordination of the central magnesium with the imidazolyl moiety of a peptidyl histidine residue, hydrogen bonding of the peripheral carbonyl groups with functional groups in a neighboring environment and π–π interaction of bacteriochlorin skeletal systems (2). A large number of BChl-*c*/*d*/*e*/*f* molecules self-aggregated via a specific combination of coordination with hydrogen bonding and π–π stacking in chlorosomes of green photosynthetic bacteria to form efficiently light-harvesting complexes which are useful for living under an extremely dim light (3). Some Chl-*a* and/or *b* molecules interact in light-harvesting complex II (LHCII) as a peripheral antenna of photosystem (PS) II in oxygenic higher plants (4).

*Corresponding author email: tamiaki@fc.ritsumei.ac.jp (Hitoshi Tamiaki)

In bacterial RCs (=BRCs), two BChl molecules including BChls-*a*/*b*/*g* are tightly stacked to give a special dimer, which functions as a primary electron donor (5). The intramolecular interaction in PSII-type BRCs of purple bacteria and filamentous anoxygenic phototrophs would be stronger than that in the other PSI type of green sulfur bacteria and heliobacteria. In RCs in oxygenic phototrophs, two Chl molecules including Chls-*a*/*d* make a primary electron donor, where they interacted with each other more loosely than in BRCs. Furthermore, interaction between the Chl-*a* molecules in the RC of PSII (P680) is weaker than that in PSI (P700).

In the above systems, most (B)Chl pigments excitonically interact to give new electronic absorption bands at longer wavelengths than the composite monomeric maxima. The special dimer of BChl-*a* molecules in BRCs of purple bacteria usually affords a redmost (Qy) band at 865 nm, while the Qy maximum of monomeric BChl-*a* in diethyl ether is situated at 771 nm (6). The bathochromic shift is ascribable to the slipped-face interaction of chlorophyllous π-systems, *i.e.* J-type aggregation.

As the primary electron donor of most (B)RCs, the same (B)Chl molecules make a dimer: Chl-*a* in PSII, BChl-*a*/*b* and Zn-BChl-*a* in PSII-type BRC and the 13^2-epimeric BChl-*a*′/*g*′ in PSI-type BRC (7). In PSI, Chl-*a* and Chl-*a*′ stereoisomers are dimerized to form the primary electron donor in the RC. Moreover, two structurally different Chl-*a* and Chl-*b* yield an excitonically coupled dimeric species in LHCII.

Many models of the chlorophyllous dimers mentioned above are available in the literature (8). Magnesium or zinc pyropheophorbide-*a* dyad possessing an ethylene glycol diester linkage was reported to take a folded conformer in 1% (v/v) methanol and benzene as shown in Fig. 1 (9,10). Methanol molecules coordinated with the central Mg or Zn atoms of the two chlorin chromophores in a molecule. The axially ligating MeOH was hydrogen bonded with the 13-carbonyl group of the neighboring chlorin in a supramolecule. Additional stacking of chlorin π-systems resulted in the folded conformer with slipped chlorin chromophores through J-type aggregation. The same bacteriochlorin or different chlorin moieties could be utilized as similar folded systems (10,11).

Here, Chl-*b*/*b* derivative homo-dyad **1bb** as well as Chl-*a*/*b* and *b*/*d* derivative hetero-dyads **1ab** and **1bd** were prepared (see Fig. 2). Visible spectra of methanol-locked Chl dyads in a solution were compared among homo-dyads **1aa/bb/dd** and hetero-dyads **1ab/ad/bd**. The other homo-dyads **2B/C/C^r/P** consisting of bacteriochlorin, chlorin and porphyrin π-systems were

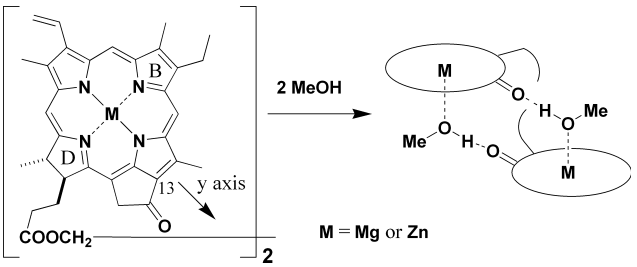

Figure 1. Synthetic magnesium or zinc pyropheophorbide-*a* dyad linked with an ethylene moiety and their intramolecular folding through coordination and hydrogen bonding with two methanol molecules.

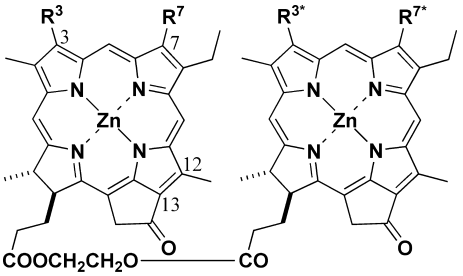

1aa: $R^3 = R^{3*} =$ CH=CH$_2$, $R^7 = R^{7*} =$ Me;
1ab: $R^3 = R^{3*} =$ CH=CH$_2$, $R^7 =$ Me, $R^{7*} =$ CHO;
1ad: $R^3 =$ CH=CH$_2$, $R^{3*} =$ CHO, $R^7 = R^{7*} =$ Me;
1bb: $R^3 = R^{3*} =$ CH=CH$_2$, $R^7 = R^{7*} =$ CHO;
1bd: $R^3 =$ CH=CH$_2$, $R^{3*} = R^7 =$ CHO, $R^{7*} =$ Me;
1dd: $R^3 = R^{3*} =$ CHO, $R^7 = R^{7*} =$ Me.

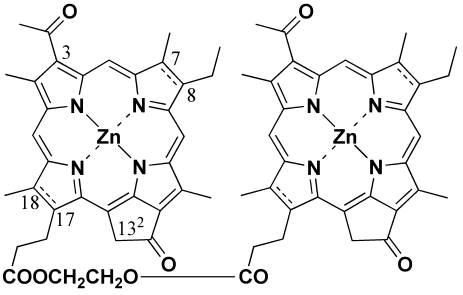

2B: C7H–C8H, C17H–C18H (7*R*,8*R*,17*S*,18*S*);
2C: C7=C8, C17H–C18H (17*S*,18*S*);
2C^r: C7H–C8H, C17=C18 (7*R*,8*R*);
2P: C7=C8, C17=C18.

Figure 2. Structures of synthetic zinc chlorophyll derivative dyads **1xy** and **2X**.

also synthesized and their intramolecular folding with methanol was investigated by electronic absorption spectroscopy.

MATERIALS AND METHODS

Apparatus. Visible absorption spectra were measured with a Hitachi U-3500 spectrometer (Tokyo, Japan). ^{1}H NMR spectra were measured at room temperature with a Bruker AC-300 (Rheinstetten, Germany) or JEOL ECA-600 spectrometer (Akishima, Japan); chemical shifts (δs) are expressed in parts per million relative to chloroform (δ = 7.26 ppm) or benzene-d_5 (δ = 7.20 ppm) as an internal reference. FT-IR spectra were recorded on a Shimadzu FTIR-8600 spectrophotometer (Kyoto, Japan); a 0.1-mm KBr cell was used for measurement of a solution sample. Mass spectra (MS) created by atmospheric pressure chemical ionization (APCI) were measured on a Shimadzu LCMS-2010EV instrument and time-of-flight (TOF) MS were obtained using direct laser desorption/ionization by a Shimadzu AXIMA-CFR plus spectrometer. Fast atom bombardment (FAB) MS were measured on a JEOL HX-100 spectrometer; the samples were dissolved in chloroform and *m*-nitrobenzyl alcohol was used as the matrix. High-resolution MS were recorded on a Bruker micrOTOF II spectrometer; APCI and positive mode in a methanol solution. High-performance liquid chromatography (HPLC) was performed on a packed octadecylated column (Cosmosil 5C$_{18}$AR-II; Nacalai Tesque, Kyoto, Japan) with a Shimadzu LC-10ADvp pump and SPD-M10Avp photodiode-array detector.

Materials. Dichloromethane for esterification was freshly distilled over CaH_2 before use. Benzene and dichloromethane for measurements of electronic and infrared absorption spectra, respectively, were purchased from Nacalai Tesque (spectroscopy grade). Flash column chromatography (FCC) was carried out on silica gel (Kieselgel 60, 9358; Merck, Darmstadt, Germany).

Methyl pyropheophorbide-*a* (**5a**) (12,13), methyl pyropheophorbide-*b* (**5b**) (14), methyl pyropheophorbide-*d* (**5d**) (15,16), methyl pyrobacteriopheophorbide-*a* (**5B**) (17), methyl 3-acetyl-3-devinyl-pyropheophorbide-*a* (**5C**) (18), methyl 17,18-didehydro-pyrobacteriopheophorbide-*a* (**5C^r**) (19), pyropheophorbide-*a* (**6a**) (20), pyropheophorbide-*d* (**6d**) (21), 2-hydroxyethyl pyropheophorbide-*a* (**7a**) (10), 2-hydroxyethyl pyropheophorbide-*d* (**7d**) (10), 2-hydroxyethyl pyrobacteriopheophorbide-*a* (**7B**) (22), ethylene bis(pyropheophorbide-*a*) (**8aa**) (10), ethylene pyropheophorbide-*a* pyropheophorbide-*d* (**8ad**) (10), ethylene bis(pyropheophorbide-*d*) (**8dd**) (10), ethylene bis(pyrobacteriopheophorbide-*a*) (**8BB**) (22), ethylene bis(zinc pyropheophorbide-*a*) (**1aa**) (10), ethylene zinc pyropheophorbide-*a* zinc pyropheophorbide-*d* (**1ad**) (10), ethylene bis (zinc pyropheophorbide-*d*) (**1dd**) (10), zinc methyl pyropheophorbide-*a* (**3a**) (23), zinc methyl pyropheophorbide-*d* (**3d**) (10), zinc methyl pyrobacteriopheophorbide-*a* (**3B**) (18), zinc methyl 3-acetyl-3-devinyl-pyropheophorbide-*a* (**3C**) (18) and zinc methyl 3-acetyl-3-devinyl-pyroprotopheophorbide-*a* (**3P**) (18) were prepared according to reported procedures.

Synthetic procedures of Chl derivative dyads are described in the next section, and their spectral data and those of their precursors are available in electronic supporting information. All the reactions were done under N_2 in the dark.

Hydrolysis. Methyl ester **5** (25 μmol) was dissolved in aqueous concentrated HCl (10 mL) at 0°C. The reaction mixture was stirred at room temperature for a few hours, poured into ice water and extracted with chloroform. The organic layer was washed with water, dried over Na_2SO_4 and filtered. After evaporation of the solvent, recrystallization from dichloromethane and hexane gave the corresponding carboxylic acid **6**. Isolated yields were 100% (**6a**), 76% (**6b**), 83% (**6d**), 86% (**6B**), 87% (**6C**) and 99% (**6C^r**).

Ethylene glycol mono-esterification. To an ice-chilled mixture of ethylene glycol (10 mL) and methyl ester **5** (25 μmol) was added concentrated H_2SO_4 (1 mL). The reaction mixture was stirred at room temperature for 5 h, poured into ice water and extracted with dichloromethane. The organic layer was washed with aqueous 4% $NaHCO_3$ and water, dried over Na_2SO_4 and filtered. After evaporation of the solvent, the residue was purified by FCC with 1.5–2% methanol and dichloromethane and successive recrystallization from dichloromethane and hexane gave the corresponding mono-ester **7**. In a 3-acetylated compound, the treatment of a stirred acetone solution (10 mL) of the above residue with aqueous 4% HCl (10 mL) at room temperature for 15 min was necessary for deprotection of its partially produced acetal before FCC purification. Isolated yields were 91% (**7a**), 81% (**7b**), 92% (**7d**), 81% (**7B**), 48% (**7C**) and 73% (**7C^r**).

Ethylene glycol diesterification. To a dry dichloromethane solution (20 mL) of free 17-propionic acid **6** (carboxylic acid component, 10 μmol) and ethylene glycol monoester **7** (alcohol component, 9 μmol) were added 1-[3-(*N*,*N*-dimethylamino)propyl]-3-ethylcarbodiimide hydrochloride (EDC·HCl, 3.8 mg, 20 μmol) and 4-(*N*,*N*-dimethylamino)pyridine (DMAP, 4.9 mg, 40 μmol) at 0°C. The reaction mixture was stirred at room temperature for 1 day, poured into ice-chilled aqueous 2% HCl and extracted with dichloromethane. The organic layer was washed with aqueous 4% $NaHCO_3$ and water, dried over Na_2SO_4 and filtered. After evaporation of the solvent, the residue was purified by FCC with 1–2% methanol and dichloromethane and successive recrystallization from dichloromethane and hexane (or dichloromethane and methanol) gave the corresponding diester **8**. Isolated yields were 85% (**8aa**), 57% (**8ab** from

6a and **7b**), 72% (**8ad** from **6a** and **7d**), 80% (**8ad** from **6d** and **7a**), 59% (**8bb**), 88% (**8bd** from **6b** and **7d**), 71% (**8dd**), 43% (**8BB**), 47% (**8CC**) and 87% (**8C^{r}C^{r}**).

Zinc metallation. A methanol solution (1 mL) saturated with Zn $(OAc)_2{\cdot}2H_2O$ was added to a dichloromethane solution (10 mL) of a free base **5** or **8** (10 μmol) and stirred at room temperature overnight. The reaction mixture was poured into aqueous 4% $NaHCO_3$ and extracted with dichloromethane. The organic layer was washed with water, dried over Na_2SO_4 and filtered. After the solvent was evaporated, the residue was purified with recrystallization from dichloromethane and hexane (or dichloromethane and methanol) and/or HPLC (column: Cosmosil $5C_{18}$-AR-II 10 $\phi \times 250$ mm; eluent: methanol and 0–13% water; flow rate: 2.0 mL min^{-1}) to give the corresponding zinc complexes **1**–**3**. For the metallation of a bacteriochlorin chromophore (in **5B** and **8BB**), refluxing in chloroform was used instead of stirring in dichloromethane at room temperature.

DDQ oxidation of zinc chlorin to zinc porphyrin. To a stirred acetone solution (50 mL) of zinc chlorin **2C** or **3C** (5 μmol) was added an acetone solution (1 mL) of 2,3-dichloro-5,6-dicyano-1,4-benzoquinone (DDQ, 10 μmol) over 30 min at room temperature. After stirred additionally for 10 min, the mixture was poured into aqueous 4% $NaHCO_3$ and extracted with chloroform. The organic layer was washed with water, dried over Na_2SO_4 and filtered. After the solvent was evaporated, recrystallization from dichloromethane and methanol and/or HPLC (vide supra) gave the corresponding zinc porphyrin **2P** or **3P**.

RESULTS AND DISCUSSION

Synthesis of zinc Chl dyads and their monomers

Zinc (B)Chl derivative dyads **1xy** and **2X** were prepared according to similar procedures reported previously (10) (except for the synthesis of ethylene glycol monoesters **7y**) and their synthetic route is shown in Fig. 3. Methyl ester **5x** was hydrolyzed by action of hydrochloric acid to give carboxylic acid **6x** [pathway (i) in Fig. 3], while the same methyl ester was directly transesterified to ethylene glycol monoester **7y** by its reaction with ethylene glycol in the presence of concentrated sulfuric acid [pathway (ii)] (15). During the transesterification, the 3-acetyl group in **5/7B** and **5/7C$^{(r)}$** was partially acetalized and the cyclic 5-membered ethylene acetal of the products could be converted to the ketone forms **7B** and **7C$^{(r)}$** by further treatment of an aqueous acidic solution. Carboxylic acid **6x** was esterified with alcohol **7y** by action of water-soluble carbodiimide (EDC) as a coupling reagent and DMAP as a coupling accelerator as well as a base to afford ethylene glycol diester **8xy** [pathway (iii)]. Finally, free base forms in the resulting Chl derivative dyads **8xy** were doubly zinc-metallated by standard procedure to give the corresponding zinc complexes **1xy** and **2X** (=**1XX**) [pathway (iv)]. All the present chlorins **8xy** were readily zinc metallated to **1xy** and **2C$^{(r)}$** with stirring at room temperature, but reflux in chloroform at 61°C was necessary for the complete metallation of bacteriochlorin **8BB** to **2B** due to its lower reactivity than any other chlorins (24). Similarly, methyl ester **5x** was zinc metallated to zinc Chl derivative **3z** as monomeric species (see Fig. 4, upper). All the synthetic Chl derivatives were characterized by their visible absorption, ^{1}H NMR and MS.

As zinc chlorin was easily oxidized to zinc porphyrin by action of DDQ in acetone (23), zinc Chl derivative dyad **2C** was smoothly oxidized to zinc protochlorophyll derivative dyad **2P** (Fig. 5). Following the same procedures for the synthesis of **1aa** [=**4(2)**], four zinc pyropheophorbide-*a* dyads **4(3)**–**4(6)** were prepared using oligomethylene glycol $HO(CH_2)_nOH$ (n = 3–6) instead of ethylene glycol (see Fig. 4, lower). All the present zinc complexes **1**–**4** were purified with recrystallization and/or

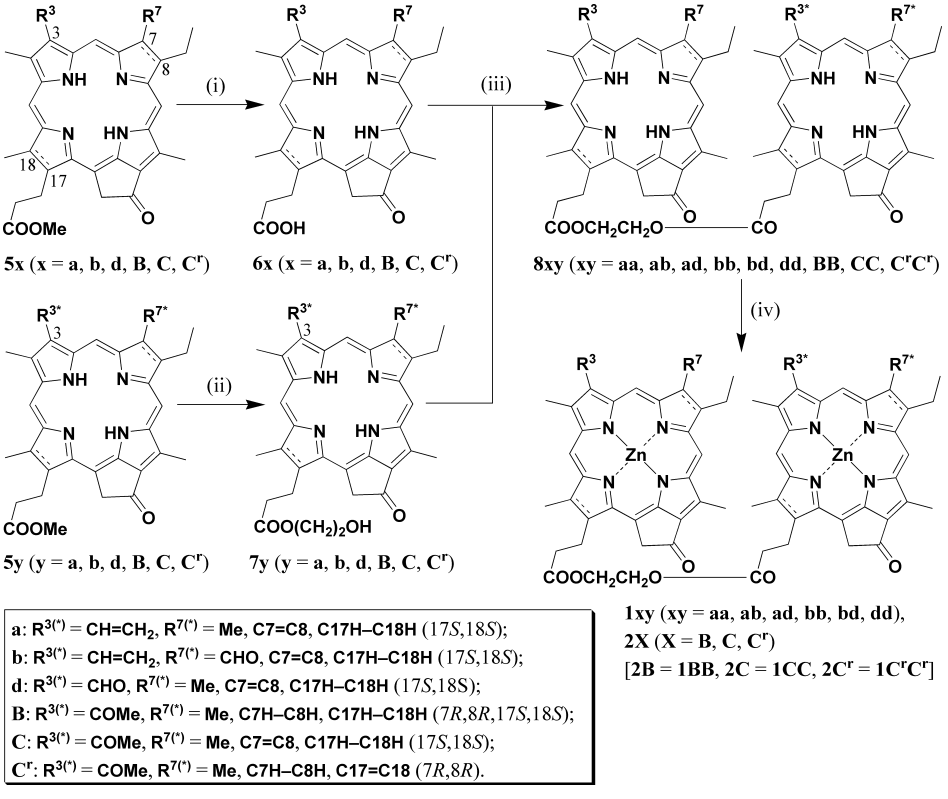

Figure 3. Synthesis of zinc (bacterio)chlorophyll derivative dyads **1xy** and **2X**: (i) conc. HCl, 0°C to rt; (ii) $HOCH_2CH_2OH$, conc. H_2SO_4, 0°C to rt (and aq. 4% HCl, acetone, rt for **B**, **C** and **C^r**); (iii) EDC·HCl, DMAP, CH_2Cl_2, 0°C to rt; and (iv) $Zn(OAc)_2{\cdot}2H_2O$, CH_3OH, CH_2Cl_2, rt ($CHCl_3$, reflux for **2B**).

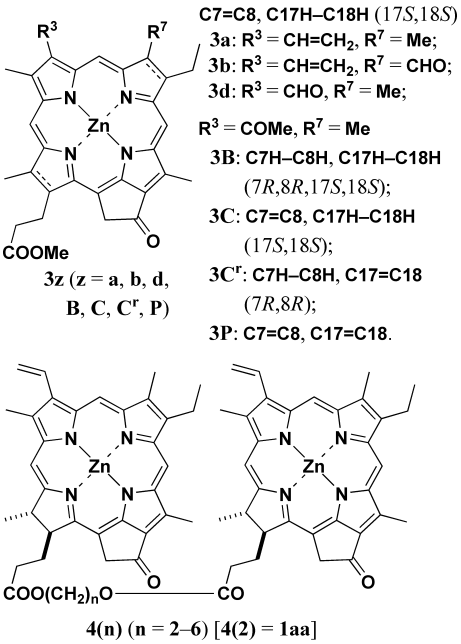

Figure 4. Structures of zinc chlorophyll derivative monomers **3z** and dyads **4(n)**.

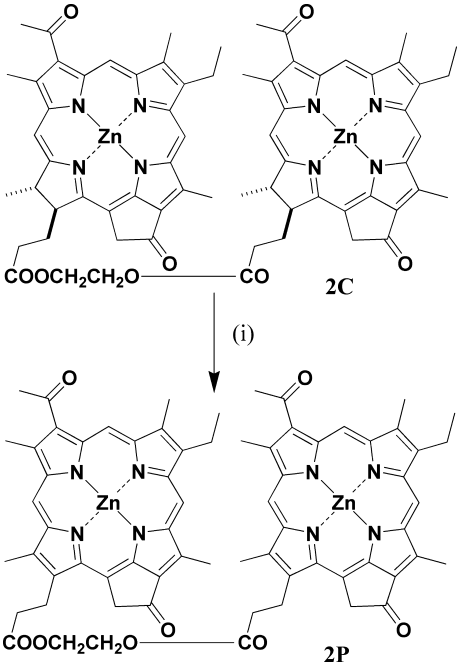

Figure 5. Synthesis of zinc protochlorophyll derivative dyad **2P**: (i) DDQ, acetone, rt.

HPLC to give analytically pure samples, which were used for measurements of their optical properties in a solution.

Folding of dyads 4(*n*) with an oligomethylene linkage in benzene containing additives

As described in the Introduction, ethylene bis(zinc pyropheophorbide-*a*) [**4(2)** = **1aa**] took a methanol-locked conformer at room temperature in 1% (v/v) methanol and benzene. The folded conformer gave redshifted electronic absorption bands, compared with those of the monomeric species (10). The redshifts were ascribable to the intramolecular J-type aggregation of the two chlorin π-systems along the *y*-axis in **4(2)**–$(MeOH)_2$ (see Fig. 1). Especially, the redshifted maximum was measured at 688 nm as the Qy peak, which moved to a longer wavelength than the 658 nm of monomer **3a** in the same solvent (see Figure S1). The elongation of oligomethylene linkage in **4(*n*)** hypsochromically shifted the Qy peak in the solution: 688 (n = 2) → 681 (3) → 680 (4) → 678 (5) → 677 nm (6). The shift would be due to the suppression of π–π stacking of chlorin chromophores with a longer spacer. The ethylene linkage (n = 2) was the most effective for the folding in five dyads **4(*n*)** (n = 2–6) examined here.

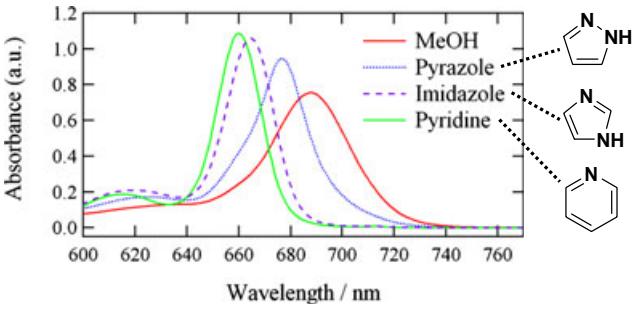

Figure 6. Qy absorption bands of zinc chlorin dyad **4(2)** (ca. 10^{-5} M) in benzene containing 1% (v/v) methanol, pyrazole, imidazole or pyridine.

Instead of methanol, pyrazole was used as the additive to give a Qy maximum at 677 nm in a benzene solution of **4(2)** (see Fig. 6). The smaller redshift is explained by the fact that a pyrazole molecule is less efficient for the bidentate binder between the chlorin chromophores than a methanol molecule: Zn···N–NH···O=C *vs* Zn···OH···O=C. Addition of imidazole molecules to a benzene solution of **4(2)** led to a much less redshifted 665-nm Qy maximum and produced a folded conformer with weakly π–π stacking via Zn···N=CH–NH···O=C. Methylation of the nitrogen atoms of pyrazole and imidazole masked the hydrogen-donating ability and gave no folded conformer, and also monodendate-binding pyridine was unable to make such a conformer. It is noteworthy that shortening of the distance between coordination and hydrogen-donating sites in additives is useful for the production of the tightly folded conformer.

Visible spectra of synthetic Chl dyads

It was reported that zinc pyropheophorbide-*a* dyad **1aa** [=**4(2)**] linked with an ethylene moiety and its 3-formyl analog **1dd** take the same folded conformer in 1% (v/v) methanol and benzene as shown in Fig. 1 and gave redshifted Qy bands: the shift values Δs = 660 cm^{-1} for **3a** → **1aa** and 630 cm^{-1} for **3d** → **1dd** (10). Ethylene bis(zinc pyropheophorbide-*b*) (**1bb**), the 7-formyl analog of **1aa**, also afforded a similar redshift in Qy bands (see Fig. 7A,C): Δ = 630 cm^{-1} for **3b** → **1bb**. The observed redshift showed that **1bb** took the same methanol-locked conformer as in **1aa** and **1dd** and the 7-formyl groups in a molecule did not disturb its formation. This is consistent with the fact that the 3-formyl group of **1dd** did not affect the folding. Chemical shifts δs of 12-methyl and 13^1-methylene protons near the 13-carbonyl group in a deuterated benzene solution of **1bb** were largely high field shifted by addition of 1% (v/v) deuterated methanol (see Figure S2): $\Delta\delta s$ = −1.94 (12-CH_3) and −0.41/−0.13 ppm

(13^1-CH_2). The vibrational stretching band of 13-C=O in a dichloromethane solution of **1bb** moved to a lower wavenumber after addition of 1%(v/v) methanol: $\nu = 1688 \rightarrow 1662$ cm^{-1}. These ^{1}H NMR and IR data support the formation of folded conformer in **1bb**–$(MeOH)_2$.

In addition to homo-dyads **1aa**, **1bb** and **1dd**, hetero-dyads **1ab**, **1ad** and **1bd** were analyzed by visible absorption spectroscopy. In 1% (v/v)MeOH–C_6H_6, **1ab** gave a Qy band at 682 nm accompanied by a shoulder at 649 nm (see Fig. 7B). The redshift from Qy maximum of **3a** (658 nm) is estimated to be 530 cm^{-1}; this value is smaller than those in homo-dyads **1aa** (660 cm^{-1}) and **1bb** (630 cm^{-1}). The decrease is ascribable to the difference in energy levels of Qy bands in the composite chlorin chromophores (658 and 640 nm, see Fig. 7A), which could interact less in the folded conformer. The shoulder observed at the blue side of the Qy band would be produced by the exciton coupling of the main Qy (0,0) band in the 7-formyl-chlorin component (as in **3b**) at 640 nm with vibrational Qy (0,1) band in the 7-methyl-chlorin component (as in **3a**) at 612 nm. The same situation has already been discussed in **1ad** (10). Two apparent Qy peaks were visible in a 1% (v/v) MeOH–C_6H_6 solution of hetero-dyad **1bd** (see Fig. 7D). One was observed at 706 nm which was shifted to a longer wavelength than that of the pyropheophorbide-*d* component (685 nm of **3d**) and the other was situated at 655 nm which was bathochromically shifted from the Qy peak of pyropheophorbide-*b* component (640 nm of **3b**). The former shift is 430 cm^{-1} and the latter is 360 cm^{-1}. These bands would be explained by similar interaction of Qy bands in the two components as in **1ab** and **1ad**: Qy (0,0) components of pyropheophorbides-*b* and *d* (640/685 nm) made the former, while Qy (0,0) of *b*-species at 640 nm and Qy (0,1) of *d*-species at 636 nm produced the latter. The redshift values are well correlated with the energy differences in between interacting components (see Fig. 8) and increase (or decrease) with an enlargement (or suppression) of overlapping of the components.

Pyropheophorbides possessing a chlorin π-system are useful for construction of the methanol-locked conformer in the dyads linked with an ethylene glycol diester. The π-conjugation of porphyrinoid components was altered and their visible spectra were measured. To avoid the substituent effect, all the homo-dyads **2X** possessing the same functional groups at the peripheral positions were prepared. Chlorin dyad **2C** (=**1CC**), the 3-acetyl analog of **1aa**, showed the redshifted Qy band at 705 nm in 1% (v/v)MeOH–C_6H_6, compared with Qy maximum at 675 nm of monomerically methanol-ligated **3C** (see Fig. 9B). The redshift value of 630 cm^{-1} was comparable to those in **3a/b/d** → **1aa/bb/dd** (660/630/630 cm^{-1}), so **2C** took the same folded conformer. It is noted that the 3-acetyl group did not disturb the formation of the methanol-locked conformer similarly as in formyl groups mentioned above.

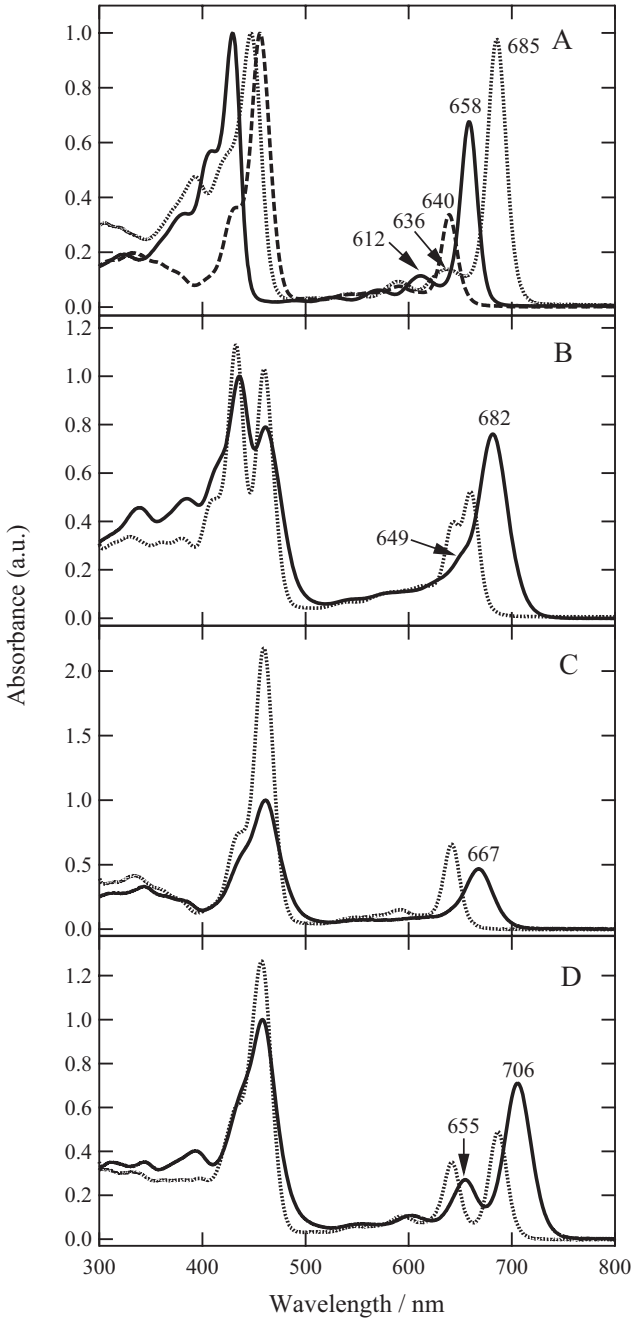

Figure 7. Electronic absorption bands of zinc chlorophyll derivatives (ca. 10^{-5} M): (A) **3a** (solid line), **3b** (broken line) and **3d** (dotted line) in benzene containing 1% (v/v) methanol; (B) **1ab**, (C) **1bb** and (D) **1bd** in benzene containing 1% (v/v) methanol (solid line) and pyridine (dotted line). Intense Soret peaks in benzene containing 1% (v/v) methanol are normalized.

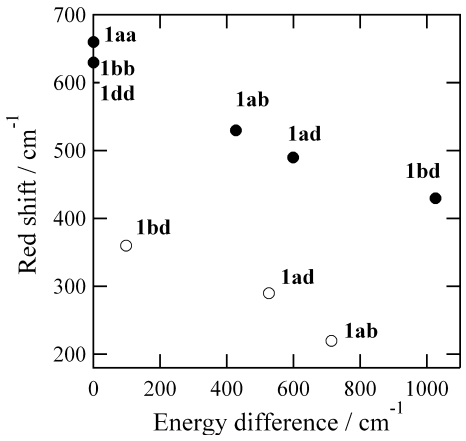

Figure 8. Dependency of redshift value in Qy bands (monomer → dyad) of zinc chlorin dyads **1xy** with energy difference of interacting Qy components in a dyad. Closed circles are based on the major band and open circles on the minor band.

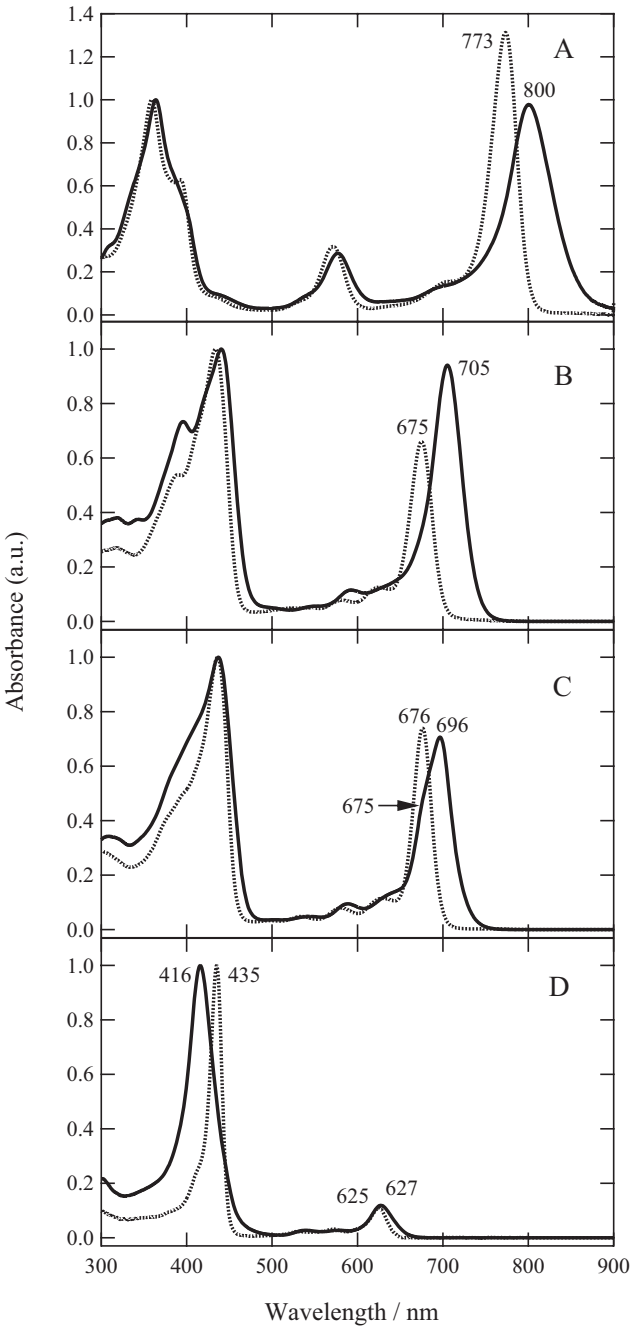

Figure 9. Electronic absorption bands of zinc chlorophyll derivatives (ca. 10^{-5} M) including monomers **3X** (dotted line) and dyads **2X** (solid line): (A) bacteriochlorins **3B/2B**; (B) chlorins **3C/2C**; (C) reverse chlorins $\mathbf{3C^r/2C^r}$; (D) porphryins **3P/2P**. Intense Soret peaks are normalized.

Bacteriochlorin dyad **2B** in 1% (v/v)MeOH–C_6H_6 gave a Qy peak at 800 nm which was shifted to a longer wavelength than that of monomer species **3B** (773 nm) as shown in Fig. 9A. The shift value of 440 cm^{-1} was smaller than that of chlorin dyad **2C**. The *trans*-hydrogenation of C7=C8 in **2C** thus suppressed the interaction of bacteriochlorin chromophores in **2B**–$(MeOH)_2$. Considering the fact that zinc bacteriochlorin had a larger coordinated ability than zinc chlorin (18), the steric hindrance at the B-ring would disturb the production of the tightly folded conformer. The redshift of ethylene bis(bacteriochlorophyllide-*a*)

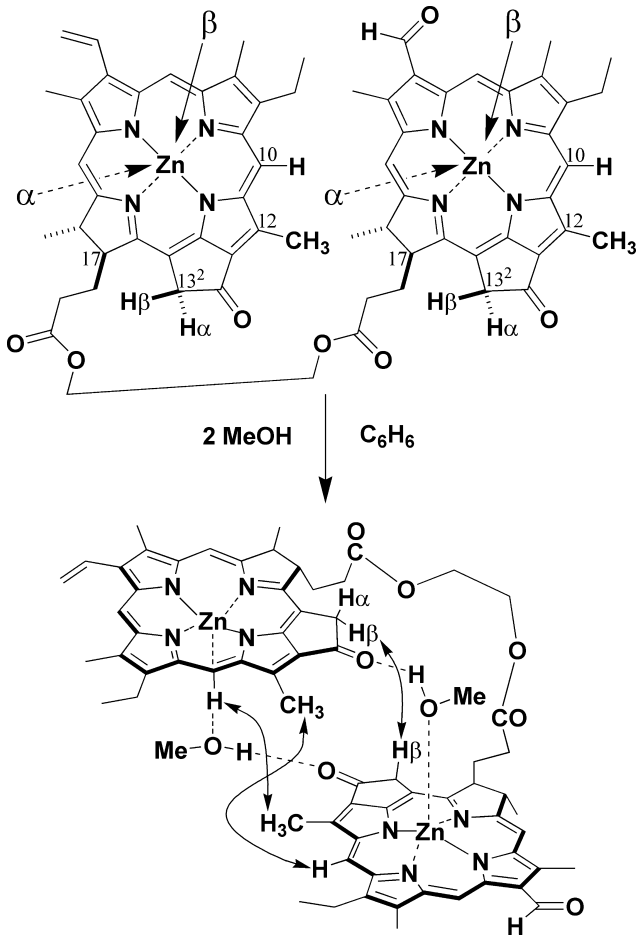

Figure 10. Molecular structure of methanol-locked conformer in zinc chlorophyll dyad **1ad**.

(=Mg analog of **2B** with 13^2-COOMe) in water-saturated benzene was reported to be 370 cm^{-1} (11), which was comparable to the present value.

To confirm the above steric effect around the B-ring, zinc chlorin dyad $\mathbf{2C^r}$ possessing 7,8-dihydroporphyrin π-systems, the regioisomer of **2C** having 17,18-dihydroporphyrins, was prepared through selective oxidation of a 7,8,17,18-tetrahydroporphyrin (=bacteriochlorin) (19); hereafter the 7,8-dihydroporphyrin is called a reverse chlorin. In 1% (v/v)MeOH–C_6H_6, reverse chlorin dyad $\mathbf{2C^r}$ showed a Qy maximum at 696 nm, while the corresponding monomer $\mathbf{3C^r}$ had a 676-nm Qy peak (see Fig. 9C). The redshift was 430 cm^{-1}, which was almost the same as the value for **2B**. Therefore, the increase in steric hindrance around the peripheral positions of the B-ring weakened the interaction of porphyrinoid moieties. The Qy band of $\mathbf{2C^r}$ had a shoulder at around 675 nm, which was assigned to the unfolded reverse chlorin. The presence of unfolded conformer indicated that the reverse chlorin partially prevented the folding of the dyad molecule. The C17=C18 double bond in the D-ring of a reverse chlorin constrained the conformational flexibility of C17-propionate residues and did not produce the folded conformer completely.

The steric effect at around the D-ring was also observed in zinc porphyrin dyad **2P**. The Qy maximum of **2P** in 1% (v/v) MeOH–C_6H_6 was almost the same as that of **3P** and the former Qy band was broadened more than the latter (see Fig. 9D). The

folded conformer of **2P** would give a red side of the Qy band. The spectral analysis indicated that **2P** partially formed the folded conformer mentioned above. The fact that a zinc porphyrin had less coordination ability than the corresponding zinc chlorin also suppressed the folding of **2P**. The Soret band of **2P** was largely shifted to a shorter wavelength than that of **3P** (435 → 416 nm), and the face-to-face folding through H-type aggregation may occur due to the extremely flat porphyrin planes.

Supramolecular structure of methanol-locked Chl dyad conformer

In the folded conformer of zinc Chl derivative dyads, the central zinc atoms were coordinated by a methanol molecule as an axial ligand to give a five-coordinated species. It is known that the chlorin π-plane of Chl derivatives has two faces, α- and β-faces (25). In the folded conformer, the five-coordinated zinc took either α- or β-ligation and four stereoisomers are proposed for the coordination sites, α,α-, α,β-, β,α- and β,β-ligation (see Fig. 10, upper). The stereochemistry in the folded conformer was identified by the following ^{1}H NMR measurements. In 1% (v/v) CD_3OD–$CDCl_3$, hetero-dyad **1ad** was analyzed by 1D and 2D NMR spectroscopy and all the peaks were assigned. From ^{1}H–^{1}H ROESY spectrum of **1ad** at −50°C, two nuclear Overhauser effect (NOE) correlations between the 10-H of pyropheophorbide-*a* moiety and 12-CH_3 of pyropheophorbide-*d* moiety and between the former 12-CH_3 and latter 10-H were clearly observed. The result showed that the two chromophores were closely situated in a molecule to give the methanol-locked conformer mentioned above. Moreover, the 13^2-H_β which was situated on the same side of the 17-propionate residue in pyropheophorbide-*a* moiety was apparently NOE correlated with the 13^2-H_β in pyropheophorbide-*d* moiety, and other NOEs were invisible for the 13^2-H_α/13^2-H_α, 13^2-H_α/13^2-H_β and 13^2-H_β/13^2-H_α in between the different chromophores This observation indicated that both the 13^2-H_β were closely situated in the folded conformer and the β-face of pyropheophorbide-*a* macrocycle interacted with the β-face of pyropheophorbide-*d* through the β-ligation of a methanol oxygen atom with a zinc atom in each zinc chlorin. The molecular structure of methanol-locked zinc Chl dyads is depicted as shown in the lower of Fig. 10 (see also the space filling model in Graphical Abstract).

CONCLUSION

Two units of zinc (B)Chl-*a*/*b*/*d* derivatives were covalently linked with a diester spacer to give homo/hetero-dyads **1xy**, **2X** and **4**(***n***). In a solution, the synthetic zinc Chl dyads were intramolecularly folded with bidentate species possessing coordinating and hydrogen-bonding abilities. The conformationally fixed supramolecules showed redshifted Qy bands through exciton coupling of the composite π-systems, compared with the corresponding monomers **3z**. The formation of such J-type aggregates was regulated by D-ring (un)saturation, spacer length and binder structure. The bathochromic shifts by the intramolecularly folding formation were sterically and electronically controlled by B-ring (un)saturation, spacer length and binder structure as well as Qy energy levels of the composite chromophores. The present supramolecules would help to understand structures and functions of closely situated (B)Chls in natural photosynthetic apparatus and their synthetic models composing of porphyrinoids.

Acknowledgements—We thank Mr. Katsunori Nishide of Ritsumeikan University for his experimental assistance. This work was partially supported by Grants-in-Aid for Scientific Research (A) (no. 22245030) as well as on Innovative Areas "Artificial Photosynthesis (AnApple)" (no. 24107002) from the Japan Society for the Promotion of Science (JSPS).

SUPPORTING INFORMATION

Additional Supporting Information may be found in the online version of this article:

Figure S1. Qy absorption spectra of monomer **3a** and dyads **4(n)** (ca. 10^{-5} M) in 1% (v/v) methanol and benzene.

Figure S2. Difference between ^{1}H chemical shifts of **1bb** in C_6D_6 containing 1% (v/v) CD_3OD and C_5D_5N.

REFERENCES

1. Melkozernov, A. N. and R. E. Blankenship (2006) Photosynthetic functions of chlorophylls. In *Chlorophylls and Bacteriochlorophylls: Biochemistry, Biophysics, Functions and Applications*, (Edited by B. Grimm, R. J. Porra, W. Rüdiger and H. Scheer), pp. 397–412. Springer, The Netherlands.
2. Cogdell, R. J., A. Gall and J. Köhler (2006) The architecture and function of the light-harvesting apparatus of purple bacteria: from single molecules to in vivo membrane. *Q. Rev. Biophys.* **39**, 227–324.
3. Orf, G. S. and R. E. Blankenship (2013) Chlorosome antenna complexes from green photosynthetic bacteria. *Photosynth. Res*. doi:10.1007/s11120-013-9869-3.
4. Liu, Z. and W. Chang (2008) Structure of the light-harvesting complex II. *In Photosynthetic Protein Complexes: A Structural Approach*, (Edited by P. Fromme), pp. 217–242. Wiley, Weinheim.
5. Tamiaki, H., R. Shibata and T. Mizoguchi (2007) The 17-propionate function of (bacterio)chlorophylls: biological implication of their long esterifying chains in photosynthetic systems. *Photochem. Photobiol.* **83**, 152–162.
6. Tamiaki, H. and M. Kunieda (2011) Photochemistry of chlorophylls and their synthetic analogs. In *Handbook of Porphyrin Science*, (Edited by K. M. Kadish, K. M. Smith and R. Guilard), Vol. 11, pp. 223–290. World Scientific, Singapore.
7. Ohashi, S., T. Iemura, N. Okada, S. Itoh, H. Furukawa, M. Okuda, M. Ohnishi-Kameyama, T. Ogawa, H. Miyashita, T. Watanabe, S. Itoh, H. Oh-oka, K. Inoue and M. Kobayashi (2010) An overview on chlorophylls and quinones in the photosystem I-type reaction centers. *Photosynth. Res.* **104**, 305–319.
8. Gunderson, V. L. and M. R. Wasielewski (2012) Supramolecular chlorophyll assemblies for artificial photosynthesis. In *Handbook of Porphyrin Science*, (Edited by K. M. Kadish, K. M. Smith and R. Guilard), Vol. 20, pp. 45–105. World Scientific, Singapore.
9. Boxer, S. G. and G. L. Closs (1976) A covalently bound dimeric derivative of pyrochlorophyllide *a*. A possible model for reaction center chlorophyll. *J. Am. Chem. Soc.* **98**, 5406–5408.
10. Tamiaki, H., K. Fukai, H. Shimazu, K. Nishide, Y. Shibata, S. Itoh and M. Kunieda (2008) Covalently linked zinc chlorophyll dimers as a model of a chlorophyllous pair in photosynthetic reaction centers. *Photochem. Photobiol. Sci.* **7**, 1231–1237.
11. Wasielewski, M. R., U. H. Smith, B. T. Cope and J. J. Katz (1977) A synthetic biomimetic model of special pair bacteriochlorophyll a. *J. Am. Chem. Soc.* **99**, 4172–4173.
12. Smith, K. M., D. A. Goff and D. J. Simpson (1985) *Meso* substitution of chlorophyll derivatives: direct route for transformation of bacteriopheophorbides *d* into bacteriopheophorbides *c*. *J. Am. Chem. Soc.* **107**, 4946–4954.

13. Tamiaki, H., S. Takeuchi, S. Tsudzuki, T. Miyatake and R. Tanikaga (1998) Self-aggregation of synthetic zinc chlorins with a chiral 1-hydroxyethyl group as a model for *in vivo* epimeric bacteriochlorophyll-*c* and *d* aggregates. *Tetrahedron* **54**, 6699–6718.
14. Tamiaki, H., M. Kubo and T. Oba (2000) Synthesis and self-assembly of zinc methyl bacteriopheophorbide-*f* and its homolog. *Tetrahedron* **56**, 6245–6257.
15. Tamiaki, H., M. Amakawa, Y. Shimono, R. Tanikaga, A. R. Holzwarth and K. Schaffner (1996) Synthetic zinc and magnesium chlorin aggregates as models for supramolecular antenna complexes in chlorosomes of green photosynthetic bacteria. *Photochem. Photobiol.* **63**, 92–99.
16. Tamiaki, H., S. Miyata, Y. Kureishi and R. Tanikaga (1996) Aggregation of synthetic zinc chlorins with several esterified alkyl chains as models of bacteriochlorophyll-*c* homologs. *Tetrahedron* **52**, 12421–12432.
17. Tamiaki, H., M. Kouraba, K. Takeda, S. Kondo and R. Tanikaga (1998) Asymmetric synthesis of methyl bacteriopheophorbide-*d* and analogues by stereoselective reduction of the 3-acetyl to the 3-(1-hydroxyethyl) group. *Tetrahedron: Asymmetry* **9**, 2101–2111.
18. Tamiaki, H., S. Yagai and T. Miyatake (1998) Synthetic zinc tetrapyrroles complexing with pyridine as a single axial ligand. *Bioorg. Med. Chem.* **6**, 2171–2178.
19. Liu, C., M. P. Dobhal, M. Ethirajan, J. R. Missert, R. K. Pandey, S. Balasubramanian, D. K. Sukumaran, M. Zhang, K. M. Kadish, K. Ohkubo and S. Fukuzumi (2008) Highly selective synthesis of the ring-B reduced chlorins by ferric chloride-mediated oxidation of bacteriochlorins: Effects of the fused imide vs isocyclic ring on photophysical and electrochemical properties. *J. Am. Chem. Soc.* **130**, 14311–14323.
20. Wasielewski, M. R. and W. A. Svec (1980) Synthesis of covalently linked dimeric derivatives of chlorophyll *a*, pyrochlorophyll *a*, chlorophyll *b*, and bacteriochlorophyll *a*. *J. Org. Chem.* **45**, 1969–1974.
21. Kosaka, N. and H. Tamiaki (2004) Synthesis of a novel cyclic chlorophyll hetero-dyad as a model compound for stacked chlorophylls found in photosynthetic systems. *Eur. J. Org. Chem.* 2325–2330.
22. Miyatake, T., H. Tamiaki, A. R. Holzwarth and K. Schaffner (1999) Artificial light-harvesting antennae: Singlet excitation energy transfer from zinc chlorin aggregate to bacteriochlorin in homogeneous hexane solution. *Photochem. Photobiol.* **69**, 448–456.
23. Tamiaki, H., T. Watanabe and T. Miyatake (1999) Facile synthesis of 13^1-oxo-porphyrins possessing reactive 3-vinyl or 3-formyl group, protochlorophyll-*ald* derivatives by 17,18-dehydrogenation of chlorins. *J. Porphyrins Phthalocyanines* **3**, 45–52.
24. Chen, C.-Y., E. Sun, D. Fan, M. Taniguchi, B. E. McDowell, E. Yang, J. R. Diers, D. F. Bocian, D. Holten and J. S. Lindsey (2012) Synthesis and physicochemical properties of metallobacteriochlorins. *Inorg. Chem.* **51**, 9443–9464.
25. Oba, T. and H. Tamiaki (2005) Effects of peripheral substituents on diastereoselectivity of the fifth ligand-binding to chlorophylls, and nomenclature of the asymmetric axial coordination sites. *Bioorg. Med. Chem.* **13**, 5733–5739.